

Decoding Potential Mechanism of Cucurbitacin IIa Treatment on Lyme Neuroborreliosis Through Integrating Network Pharmacology-Molecular Docking Technique and Cell Experiment

Yuxin Fan^{1,2,3*}, Fukai Bao^{1,2**}, Hanxin Wu¹, Li Peng¹, Liangyu Zhu¹, Aihua Liu^{1**}

¹Yunnan Province Key Laboratory of Children's Major Diseases Research, Department of Pathogen and Immunology, School of Basic Medicine, Kunming Medical University, Kunming 650030, Yunnan, China

²Research Center, Baoshan People's Hospital, Baoshan 678100, Yunnan, China

³The People's Hospital of Leshan, Leshan 614003, Sichuan, China

Abstract

Introduction: Cucurbitacin IIa (CuIIa), one of the most important active components of *Cucurbitaceae* plants, has a wide range of pharmacological effects. However, the mechanisms underlying its effects on Lyme neuroborreliosis (LNB) remain unclear. This study aimed to elucidate the potential mechanisms of CuIIa activity against LNB.

Methods and Results: Potential CuIIa targets were obtained from the PharmMapper, Swiss Target Prediction, and Batman-Traditional Chinese medicine databases. LNB-associated genes were obtained from OMIM, GeneCards, and DisGeNET. Disease-drug intersection targets were identified using Venny. Protein-protein interaction (PPI) networks were constructed using STRING. Gene ontology (GO) and Kyoto Encyclopedia of Genes and Genomes (KEGG) pathway enrichment analyses were done on the Database for Annotation, Visualization, and Integrated Discovery (DAVID). A drug-target-pathway-disease network was constructed and Autodock software was used to verify molecular docking between active ingredients and the core targets. Finally, the key targets were experimentally validated.

A total of 574 CuIIa targets and 73 LNB-associated genes were identified, and 13 genes were common between the 2 groups. By constructing a PPI network for key targets, the top 10 core target genes were *MMP9*, *TNF*, *ALB*, *CTSG*, *TGFB1*, *CCL2*, *IL4*, *CRP*, *CCL3*, and *CCL5*. GO functional enrichment and KEGG pathway analyses identified 118 entries and 110 pathways, respectively. Molecular docking results showed that CuIIa binds to key important targets in the core network with high affinity. Validation analyses of the key targets, *CCL2* and *CCL5*, showed that CuIIa decreased their expression in a concentration-dependent manner.

Conclusion: This study revealed the potential mechanism of CuIIa activity against Lyme neuroborreliosis. Our preliminary findings using molecular docking modeling and experimental validation provide a basis for future clinical CuIIa applications. (International Journal of Biomedicine. 2025;15(4):715-721.)

Keywords: Cucurbitacin IIa • Lyme neuroborreliosis • network pharmacology • enrichment analysis • chemokine • molecular docking

For citation: Fan Y, Bao F, Wu H, Peng L, Zhu L, Liu A. Decoding Potential Mechanism of Cucurbitacin IIa Treatment on Lyme Neuroborreliosis Through Integrating Network Pharmacology-Molecular Docking Technique and Cell Experiment. International Journal of Biomedicine. 2025;15(4):715-721. doi:10.21103/Article15(4)_OA11

Introduction

Lyme disease (LD) is a zoonotic disease caused by the *Borrelia burgdorferi* (*Bb*) infection, which is transmitted through tick bites.¹ In the early stage of LD, *Bb* can cross the blood-brain barrier and enter the central nervous system. Due to its high neurotropism, *Bb* can remain in the central or peripheral nervous system for an extended period, causing various neuropathies. Neurological manifestations are reported in up to 12% of patients with LD.² Lyme neuroborreliosis

(LNB) is an infectious disease of the nervous system caused by *Bb* infection.² The first case of LNB was reported in 1922 by Garin and Bujadoux, who described a patient in France who developed meningitis and erythema after being bitten by a tick.² Later, many cases with similar complications were reported, often presenting with meningitis, myelitis, painful radiculitis, cerebral palsy, and headache, with severe cases progressing to facial paralysis and dementia. The most common neurological symptoms of LNB are painful meningoencephalitis (Bannwarth syndrome) and lymphocytic meningitis.² Lyme disease is

mainly treated with antibiotics. Treatment with doxycycline or amoxicillin for 14–21 days is recommended for patients with early or early spread without nervous system involvement. Up to 28 days of antibiotic therapy are recommended for cases involving the central nervous system.^{3,4} Although early LD can be successfully treated with doxycycline or amoxicillin, advanced LD can be refractory to antibiotic treatment when accompanied by arthritis and neurological symptoms. About 10% of LD patients experience persistent symptoms that do not resolve for several months after one or more rounds of antibiotic therapy.⁵ Thus, more effective treatments for insensitive LNB, including anti-inflammatory drugs and especially antibiotics, are urgently needed.

Cucurbitacin IIa (CuIIa), a tetracyclic triterpenoid compound, is a key active component of the plant species *Cucurbita*. Yunnan people use the root of snow bile tuber to treat various diseases, including dysentery, enteritis, bronchitis, and acute tonsillitis. CuIIa has various effects, including lowering fever, detoxification, antibacterial, and anti-inflammatory properties.^{6,7} Studies have shown that CuIIa also exhibits anti-hepatitis B virus effects, inhibits HIV replication, and possesses antidepressant properties.⁸ Using high-performance liquid chromatography, a study of the antidepressant effects of CuIIa showed that it can cross the blood–brain barrier.⁹ CuIIa-containing drugs, which have high developmental value, have been used clinically in China, and they can modulate a variety of signaling and metabolic pathways.

With the availability of large datasets and advances in artificial intelligence, systems biology-based network pharmacology has emerged as a valuable tool for studying the mechanisms of action of drugs. Using network pharmacology, multivariate drug–target–pathway–disease interaction networks can be constructed, and topological analysis of such networks can reveal the mechanisms of drug action against diseases.¹⁰ In this study, we employed network pharmacology to uncover novel potential strategies for LNB treatment. We predicted the mechanisms of CuIIa activity against LNB, screened for potential CuIIa targets, and subsequently carried out experimental validation.

Materials and Methods

Flowchart of the network pharmacology analysis

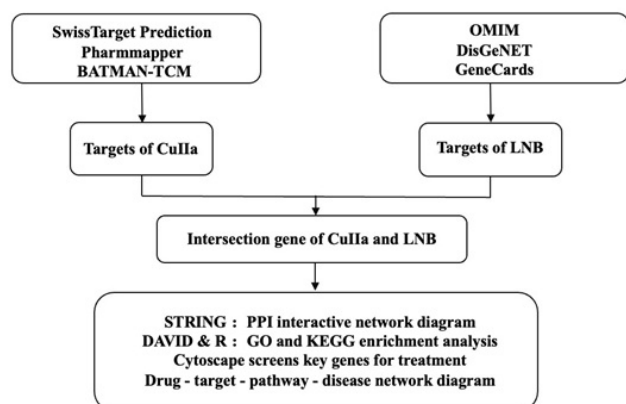


Figure 1. Schematic representation of the network pharmacology strategy used to predict the mechanisms of CuIIa activity against LNB.

Prediction of Potential CuIIa Targets

The 2D structure of CuIIa was obtained from PubChem (<https://pubchem.ncbi.nlm.nih.gov/>),¹¹ saved in SDF file format. It was imported into the SwissTargetPrediction (<http://www.swisstargetprediction.ch/>) database to select the species *Homo sapiens* and the top 100 targets. Import PharmMapper (<http://www.lilab-ecust.cn/pharmmapper/index.html>) database and select Human Protein Targets Only, number of Reserved Matched Targets (Max 1,000). 300 targets were selected for prediction.^{12,13} Moreover, the BATMAN-TCM database (<http://bionet.ncpsb.org/batman-tcm/>) was used to identify potential CuIIa targets¹⁴ using scores of >5 and $P < 0.05$ as cutoff thresholds. Finally, the potential targets identified using the three databases were combined.

Prediction of LNB-Associated Genes

Next, to identify LNB-associated genes, DisGeNET (Score > 0.01) (<https://www.disgenet.org/home/>), GeneCards (Relevance score \geq mean value) (<http://www.genecards.org/>), and OMIM databases (<https://omim.org/>) were searched for disease-associated targets using “Lyme neuroborreliosis” as the keyword.^{15–17} The potential targets identified from the three databases were then combined.

Target Gene Annotation

Potential CuIIa targets and LNB-associated genes were annotated on UniProt (<https://www.uniprot.org/>).¹⁸

Identification of Intersection Targets

Genes that were common between the CuIIa target and the LNB-associated lists were identified using Venny 2.1.0 (<https://bioinfo.gp.cnb.csic.es/tools/venny/index.html>).¹⁹

Construction of a PPI Network of the Key Genes and Identification of Hub Genes

To determine the relationship between the intersecting target proteins, the key genes that may mediate the effects of CuIIa on LNB were subjected to protein-protein interaction (PPI) network analysis using STRING (<https://cn.string-db.org/>) with a reliability threshold of >0.4 as the cutoff.²⁰ Next, the network was visualized using Cytoscape (3.8.0). The top 10 interacting genes were then identified as hub genes and visualized using the Cytoscape CytoHubba plugin.²¹

GO and KEGG Pathway Enrichment Analysis

The intersection genes of the LNB treatment by CuIIa were imported into DAVID (<https://david.ncifcrf.gov/>) and subjected to GO and KEGG pathway enrichment analyses.²² The GO and KEGG pathway enrichment results were then visualized using the “clusterProfiler” package in R (version 4.1.3), utilizing bar graphs and bubble plots.

Construction of the Drug–Target–Pathway–Disease Network Map

A drug–target–pathway–disease network was constructed to elucidate the synergistic mechanisms of the multi-target and multi-pathway effects of CuIIa against LNB. The top 20 KEGG pathways and the 12 co-regulatory targets associated with the pathways were selected for network file creation. They were then imported into Cytoscape (3.8.0) for network visualization.

Molecular Docking

Based on the degree value, two key target proteins were selected from the top five targets in the PPI network and used for molecular docking analysis with corresponding drugs, which also included three positive drugs: doxycycline, ceftriaxone, and cefotaxime. Through the PubChem database (<https://pubchem.ncbi.nlm.nih.gov/>), access to medicines, 2D structure, and application of OpenBabel software into 3D structure,^{11,23} select the core target proteins of the human species with high resolution in the Protein Data Bank (PDB) database (<https://www.rcsb.org/>), and download the 3D model structure of the proteins.²⁴ Pymol 2.4.0 software was then used to remove water molecules and ligands from the core proteins. The completed core protein receptor and drug ligand files were imported into AutoDock Tools 1.5.7, a molecular docking software used to determine the rationality of target genes, and subjected to hydrogenation and charge calculation analyses using AutoDock 4.²⁵ The above two files were converted into. pdbqt format and imported into Autodock for molecular docking analysis of the interaction between drugs and the core proteins. The analysis results were then visualized using Pymol 2.4.0 software.²⁶

Experimental Validation of the Key Targets

Cell culture

CuIIa was purchased from Yunnan Yizhihao Pharmaceutical Co. Because astrocytes are the most abundant cells in the central nervous system, the astrocyte cell line U251 was selected for the validation experiments. The U251 cells were obtained from Kunming Institute of Zoology, Chinese Academy of Sciences, Kunming, China, and cultured in DMEM (Gibco) supplemented with 10% fetal bovine serum, 100 U/mL penicillin, and 100 µg/mL streptomycin in a humidified incubator at 37 °C, 5% CO₂. To count cells, cell suspensions were mixed with trypan Blue at a 1:1 ratio, and the cells were counted using a Countstar cell counter. The U251 cells were seeded into 6-well plates at a density of 4×10⁵ cells/well (in 2 mL) and treated with the negative control (PBS), *Bb*, *Bb*+1 µM CuIIa, *Bb*+25 µM CuIIa, and *Bb*+50 µM CuIIa for 6, 12, and 24 hours. The cells were then lysed using RNAiso Plus reagent (TaKaRa) and stored at -80 °C until RNA extraction. Cell culture supernatants were collected and stored at -20 °C until ELISA was carried out.

RT-qPCR

Total RNA was extracted from cells using the RNAiso Plus reagent (TaKaRa, Japan) according to the manufacturer's instructions. A PrimeScript RT Reagent Kit (TaKaRa, Japan) with a gDNA eraser was used for cDNA synthesis, following the manufacturer's protocol. RT-qPCR analysis was done using SYBR Premix Ex Taq (TaKaRa), and relative gene expression was determined using the 2^{-ΔΔC_t} method (Livak method) using GAPDH as the reference gene. Primer sequences are shown in Table 1.

ELISA

The effect of CuIIa on CCL2 expression was analyzed using ELISA and a human CXCL2 ELISA kit (Wuhan Eliret Biotechnology Co, LTD) according to the manufacturer's protocol, followed by absorbance (450 nm) reading on a Bio-Rad microplate reader (Model 680, BioRad Laboratories, Inc, Hercules, CA, USA).

Table 1.

Table of primer sequences for qPCR.

Gene	Forward primer (5'-3')	Reverse primer (5'-3')
<i>CCL2</i>	GCAGCAAGTGTCCTCCAAAGAA	TCCTGAACCCACTTCTGCTT
<i>CCL5</i>	TGGGTTCGGGAGTACATCAA	AAGAGCAAGCAGAAACAGGC
<i>GAPDH</i>	AGCCTTTCCTGTCTCTCAA	CAATGCCAGGTACATGGTG

Statistical Analyses

Statistical analyses and mapping were done using GraphPad Prism 8.4.3. Data are presented as mean ± standard error of the mean, and differences between groups were compared using two-way ANOVA. *P*<0.05 indicates statistically significant differences.

Results

Prediction of Relevant Action Targets

Potential CuIIa Targets

The 2D structure of CuIIa was obtained from PubChem (Figure 2A). Potential CuIIa drug targets were predicted on SwissTargetPrediction (100 targets) and PharmMapper (412 targets), and targets were transformed on UniProt. A total of 183 potential drug targets were predicted using the BATMAN-TCM database. Combining the factors identified from the three databases found 632 common potential drug targets.

LNB-Associated Genes

LNB-associated genes were obtained from DisGeNET (11 genes), GeneCards (60 genes), and OMIM (11 genes). Combining the genes identified from the results of the three databases found 73 common LNB-associated genes (Figure 2).

Identification of Intersection Targets

To identify key genes that may underlie the effects of CuIIa against LNB, the intersection between the potential CuIIa targets and LNB-associated genes was determined using Venny 2.0.1 (Figure 2B). This analysis identified 13 (1.9%) intersection genes (*ALB*, *GSR*, *MMP9*, *PPIA*, *CTSG*, *GPI*, *TGFB1*, *CCL2*, *CCL5*, *CRP*, *TNF*, *CCL3*, and *IL4*).

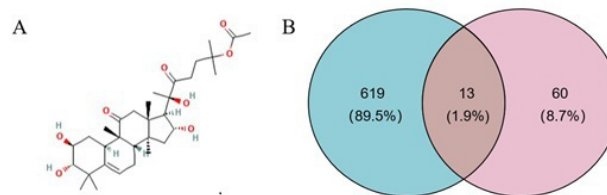


Figure 2. The 2D structure and potential targets of CuIIa. The 2D structure of CuIIa (A). A Venn diagram of the intersecting potential CuIIa targets (B).

Construction of the PPI Network

To determine the relationships between the 13 intersection genes, we subjected them to PPI network analysis using STRING (Figure 3A). The nodes on the PPI network represent the proteins, whereas the different colors of the edges

indicate various types of protein interactions. Thicker edges indicate stronger protein interactions. This analysis revealed that the PPI network consisted of 13 nodes and 46 edges, with an average node degree of 7.08 and an average local clustering coefficient of 0.859.

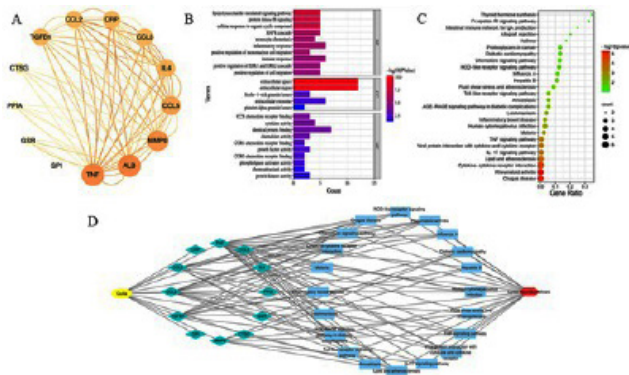


Figure 3. The CuIIa-target pathway and CuIIa-LNB interaction network. PPI network diagram (A). GO enrichment analysis results (B). The top 20 pathways identified through KEGG enrichment analysis are shown as bubble maps (C). The CuIIa-target-pathway-LNB network (D).

GO and KEGG Enrichment Analysis Results

A total of 118 results were obtained from the GO enrichment analysis, including 96 biological processes (BP), 10 cellular components (CC), and 12 molecular functions (MF) (Figure 3B). The BP terms were enriched for lipopolysaccharide-mediated signaling pathway, protein kinase B signal, cell response to organic cyclic compounds, MAPK cascade activation, monocyte chemotaxis, inflammatory response, positive regulation of monocyte migration, immune response, positive regulation of ERK1 and ERK2 cascade, and positive regulation of cell migration. The CC terms were mainly enriched for extracellular fluid, extracellular region, ficolin-1-rich granule lumen, extracellular body, and platelet α lumen. The MF terms were mainly enriched for cell surface, secretory granules, macromolecular complexes, secretory granule lumen, and blood particles.

KEGG analysis identified a total of 110 enriched pathways, and the top 20 were selected for further analysis (Table 2). These pathways were mainly associated with IL-17, TNF, MAPK, senescence in diabetic complications, Toll-like receptor, Nod-like receptor, and chemokine signaling pathways. A channel bubble map was made using R, with the bubble size corresponding to the number of genes and the bubble’s color indicating the magnitude of the *P*-value (Figure 3C).

Hub Genes for CuIIa Treatment of LNB

The 10 genes (*ALB*, *MMP9*, *CTSG*, *TGFB1*, *CCL2*, *CCL5*, *CRP*, *TNF*, *CCL3*, and *IL4*) were identified as the PPI network’s hub genes using the Cytoscape plugin cytoHubba (Figure 4A).

Construction of a CuIIa-Target-Pathway-LNB Network

The 12 key targets from the 20 main signaling pathways and the major components of their mappings were visualized on Cytoscape 3.8.0, followed by the construction of a “CuIIa-target-pathway-LNB”. This analysis identified 34 nodes (1

drug, 1 disease, 12 protein targets, and 20 pathways) and 105 edges (Figure 3D).

Table 2.
The top 20 KEGG pathways.

Pathway	<i>P</i> -value	Related genes
Rheumatoid arthritis	0.00000491	<i>CCL2</i> , <i>CCL3</i> , <i>CCL5</i> , <i>TGFB1</i> , <i>TNF</i>
Chagas disease	0.00000711	<i>CCL2</i> , <i>CCL3</i> , <i>CCL5</i> , <i>TGFB1</i> , <i>TNF</i>
Cytokine-cytokine receptor interaction	0.00002311	<i>IL4</i> , <i>CCL2</i> , <i>CCL3</i> , <i>CCL5</i> , <i>TGFB1</i> , <i>TNF</i>
Lipid and atherosclerosis	0.00013398	<i>MMP9</i> , <i>CCL2</i> , <i>CCL3</i> , <i>CCL5</i> , <i>TNF</i>
IL-17 signaling pathway	0.00022879	<i>IL4</i> , <i>MMP9</i> , <i>CCL2</i> , <i>TNF</i>
Viral protein interaction with cytokine and cytokine receptor	0.00027478	<i>CCL2</i> , <i>CCL3</i> , <i>CCL5</i> , <i>TNF</i>
TNF signaling pathway	0.00038389	<i>MMP9</i> , <i>CCL2</i> , <i>CCL5</i> , <i>TNF</i>
Malaria	0.00195561	<i>CCL2</i> , <i>TGFB1</i> , <i>TNF</i>
Human cytomegalovirus infection	0.00290129	<i>CCL2</i> , <i>CCL3</i> , <i>CCL5</i> , <i>TNF</i>
Inflammatory bowel disease	0.00328409	<i>IL4</i> , <i>TGFB1</i> , <i>TNF</i>
Leishmaniasis	0.00457921	<i>IL4</i> , <i>TGFB1</i> , <i>TNF</i>
AGE-RAGE signaling pathway in diabetic complications	0.00761674	<i>CCL2</i> , <i>TGFB1</i> , <i>TNF</i>
Amoebiasis	0.00791437	<i>CTSG</i> , <i>TGFB1</i> , <i>TNF</i>
Toll-like receptor signaling pathway	0.00821724	<i>CCL3</i> , <i>CCL5</i> , <i>TNF</i>
Fluid shear stress and atherosclerosis	0.01434047	<i>MMP9</i> , <i>CCL2</i> , <i>TNF</i>
Hepatitis B	0.01917171	<i>MMP9</i> , <i>TGFB1</i> , <i>TNF</i>
Influenza A	0.02122703	<i>CCL2</i> , <i>CCL5</i> , <i>TNF</i>
NOD-like receptor signaling pathway	0.02435339	<i>CCL2</i> , <i>CCL5</i> , <i>TNF</i>
Chemokine signaling pathway	0.02636753	<i>CCL2</i> , <i>CCL3</i> , <i>CCL5</i>
Diabetic cardiomyopathy	0.02924612	<i>GSR</i> , <i>MMP9</i> , <i>TGFB1</i>

Molecular Docking Results

Molecular docking is a widely used method in drug discovery for predicting ligand–target interactions.²⁷ Because molecular docking can also be used to estimate the ligand–receptor binding free energy by evaluating the key phenomena involved in intermolecular recognition, it can elucidate molecule–target binding modes and affinities.²⁸ This study employed a molecular docking approach to validate the core targets *CCL2* and *CCL5*, as identified by network pharmacology, for their binding to core proteins. Because ligands and receptors bind at lower energies, the

more conformationally stable they are, the likelier they are to interact. The molecular docking analysis revealed that in CCL2, CuIIa formed one hydrogen bond with ARG-328 and two hydrogen bonds with GLU-335 and LYS-326, at a binding energy of -4.82 kcal/mol. The binding energy between CuIIa and CCL5 was -5.86 kcal/mol. The binding energies of the active chemical components to the key target proteins were all less than -4 kcal/mol. The binding energy of CuIIa with CCL2 and CCL5 was higher than that of the three positive drugs (Table 3), indicating that the compound has stable receptor binding activity. The docking pattern maps between CuIIa and the CCL2 and CCL5 proteins were visualized using the Pymol software (Figure 4).

Table 3.

Docking results of core components and core target proteins.

Core element	Binding energy (kJ/mol)			
	CuIIa	Doxycycline	Ceftriaxone	Cefotaxime
CCL2	-4.82	-1.71	-2.69	-0.72
CCL5	-5.86	-3.54	-1.19	-2.73

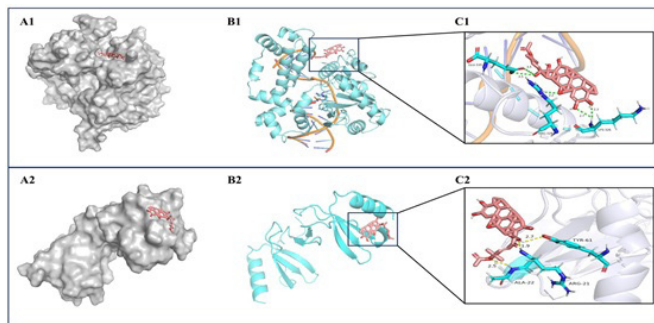


Figure 4. An illustration of the docking between CuIIa and the CCL2 and CCL5 proteins. Schematic diagram of the three-dimensional morphology of CuIIa docking with the target proteins (A). Schematic diagram of the docking site bonds between CuIIa and the target proteins (B). Schematic diagram of the docking site energy bonds of CuIIa with target proteins (C). Hydrogen bonds are represented by yellow dotted lines, with the length indicated around the lines.

Analysis of the mRNA Levels of the Key Targets, CCL2 and CCL5

RT-qPCR analysis revealed that after 24 hours of treatment, the mRNA levels of CCL5 and CCL2 in U251 cells were significantly higher in the *Bb* group when compared with the negative control group (Figure 5B–C), indicating that *Bb* significantly upregulated CCL2 and CCL5 levels. When compared with the *Bb*-treated group, treatment with CuIIa significantly suppressed the expression of CCL5 and CCL2 in a dose-dependent manner ($P < 0.01$ and $P < 0.05$). ELISA revealed that *Bb* significantly increased the protein levels of CCL2 in U251 cells, and CuIIa significantly reduced CCL2 protein levels in a dose-dependent manner when compared with the *Bb* group ($P < 0.01$ and $P < 0.05$). These results are consistent with the findings from network pharmacology.

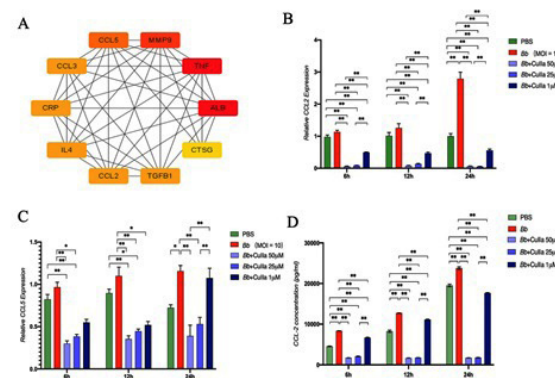


Figure 5. Hub genes of hosts infected with *Bb* infection and experimental validation. Top 10 Hub genes (A). Effect of CuIIa on CCL2 and CCL5 mRNA levels and CCL2 protein levels in the human astrocyte cell line, U251. U251 cells were treated with *Bb* (Multiplicity of infection = 10), PBS (negative control), and three drug combination groups (*Bb*+1 μ M CuIIa, *Bb*+25 μ M CuIIa, and *Bb*+50 μ M CuIIa) for 6, 12, and 24 hours. The mRNA levels of CCL2 and CCL5 (B–C) and the CCL2 protein concentrations are shown (D). Values represent means \pm standard error of the mean (* and ** indicate $P < 0.05$ and < 0.01 , respectively).

Discussion

Currently, LNB treatment is difficult because of poor antibiotic efficacy and post-treatment Lyme disease syndrome (PTLD). In some patients, PTLD is associated with persistent cognitive dysfunction, fatigue, and fibromuscular pain after antibiotic therapy. Moreover, clinical trials indicate that long-term antibiotic therapy does not appear to benefit patients with PTLD.^{2,29} Infectious Diseases Society of America guidelines do not recommend additional antibiotic therapy for patients with persistent or recurrent nonspecific symptoms, such as fatigue, pain, or cognitive impairment, following the recommended Lyme disease treatment unless there is objective evidence of reinfection or treatment failure.³⁰ CuIIa has various effects, including antibacterial, anti-inflammatory, and anti-tumor activities.^{7,31} Our unpublished data indicate that CuIIa was effective at alleviating Lyme disease symptoms. In this study, we employed network pharmacology to investigate further the mechanism underlying the effects of CuIIa against LNB.

To our knowledge, this is the first study to investigate CuIIa targets against LNB using network pharmacology and molecular docking analyses. The network pharmacology results suggest that CuIIa may improve LNB through its effects on several key genes, including *MMP9*, *TNF*, *ALB*, *CTSG*, *TGFB1*, *CCL2*, *IL4*, *CRP*, *CCL3*, and *CCL5*, as well as the modulation of various pathways, including IL-17, TNF, MAPK, aging, Toll-like receptor, nodal-like receptor, and chemokine signaling pathways. LNB pathogenesis is not fully understood, and immune-mediated neuroinflammation is thought to be the leading cause of LNB-associated nerve injury. Our GO enrichment analysis revealed that BPs were primarily enriched for inflammatory response, immune response, and monocyte chemotaxis, while MFs were enriched mainly for cytokine activity, chemokine activity, and protein kinase activity, suggesting that inflammatory responses play a crucial role in LNB. Recent studies have suggested that TLR activation and

the resulting production of pro-inflammatory chemokines and inflammatory cytokines may drive LNB inflammation.³² CuIIa may exert anti-inflammatory effects by regulating the TLR pathway. Additionally, it has also been shown that the anti-inflammatory effects of CuIIa are closely associated with the mitogen-activated protein kinase (MAPK) pathway.⁷

Among the key targets identified in this study, we focused on *CCL2* and *CCL5*, which are closely associated with LNB inflammation and may contribute to the progressive exacerbation of the LNB inflammation. Characteristic monocyte infiltration is often observed in the cerebrospinal fluid of patients with LNB; however, the mechanism of their recruitment remains unclear.^{2,33} Elevated *CCL2* and *CCL5* expression have been observed in the cerebrospinal fluid of LNB patients and in an animal model of Bb-induced mouse arthritis.³⁴ It has been demonstrated that chemokine levels, such as *CCL2*, *CCL5*, and *CCL9*, can induce monocytes and other immune cells to infiltrate inflammatory tissues, thereby exacerbating the progression of Lyme disease.³⁵ Therefore, we selected *CCL2* and *CCL5* for experimental validation. To this end, we infected the human astrocyte cell line, U251, with *Bb* and treated them with a negative control and three drug treatment groups. RT-qPCR and ELISA analyses revealed that *Bb* upregulated *CCL2* and *CCL5*, whereas CuIIa suppressed their expression in a concentration-dependent manner. These observations suggest that CuIIa might mediate its effects against LNB by targeting *CCL2* and *CCL5*. These preliminary findings highlight a potential strategy for treating antibiotic-unresponsive patients with LNB or PTLDS.

Conclusion

This study reveals the potential mechanism of CuIIa against Lyme disease. A total of 574 CuIIa targets and 73 LNB-related genes were identified. By constructing PPI networks of key targets, the top 10 core target genes were *MMP9*, *TNF*, *ALB*, *CTSG*, *TGFB1*, *CCL2*, *IL4*, *CRP*, *CCL3*, and *CCL5*. GO enrichment and KEGG pathway analysis identified 118 portals and 110 pathways, respectively. Molecular docking results show that CuIIa binds key and important targets in the core network with high affinity. Confirmatory analyses of key targets *CCL2* and *CCL5* showed that CuIIa reduced their expression in a concentration-dependent manner.

Financial Support

This work was supported by grants from the National Natural Science Foundation of China (No. 32060180, 82160304, 81860644, 81560596), Joint Special Project of Yunnan Science and Technology Department and Kunming Medical University [No.2019FE001(-002) and 2017FE467(-001)]. The funding institutions had no involvement in the design of the study or review of the manuscript.

Declaration of Competing Interest

The authors declare that there are no conflicts of interest.

Acknowledgements

The authors thank the Yunnan Province Key Laboratory for Tropical Infectious Diseases in Universities,

the Yunnan Province Integrative Innovation Center for Public Health, Diseases Prevention, and Control, Kunming Medical University, and the Yunnan Demonstration Base of International Science and Technology Cooperation for Tropical Diseases (all located in Kunming, China) for their support of this study.

Availability of data and materials

The datasets used and/or analyzed during the current study are available from the corresponding author on reasonable request.

References

1. Mead P. Epidemiology of Lyme Disease. *Infect Dis Clin North Am*. 2022 Sep;36(3):495-521. doi: 10.1016/j.idc.2022.03.004.
2. Garcia-Monco JC, Benach JL. Lyme Neuroborreliosis: Clinical Outcomes, Controversy, Pathogenesis, and Polymicrobial Infections. *Ann Neurol*. 2019 Jan;85(1):21-31. doi: 10.1002/ana.25389.
3. Bobe JR, Jutras BL, Horn EJ, Embers ME, Bailey A, Moritz RL, et al. Recent Progress in Lyme Disease and Remaining Challenges. *Front Med (Lausanne)*. 2021 Aug 18;8:666554. doi: 10.3389/fmed.2021.666554.
4. Wormser GP, Dattwyler RJ, Shapiro ED, Halperin JJ, Steere AC, Klempner MS, Krause PJ, Bakken JS, Strle F, Stanek G, Bockenstedt L, Fish D, Dumler JS, Nadelman RB. The clinical assessment, treatment, and prevention of lyme disease, human granulocytic anaplasmosis, and babesiosis: clinical practice guidelines by the Infectious Diseases Society of America. *Clin Infect Dis*. 2006 Nov 1;43(9):1089-134. doi: 10.1086/508667. Epub 2006 Oct 2. Erratum in: *Clin Infect Dis*. 2007 Oct 1;45(7):941.
5. Steere AC, Angelis SM. Therapy for Lyme arthritis: strategies for the treatment of antibiotic-refractory arthritis. *Arthritis Rheum*. 2006 Oct;54(10):3079-86. doi: 10.1002/art.22131.
6. Chen DL, Xu XD, Li RT, Wang BW, Yu M, Liu YY, Ma GX. Five New Cucurbitane-Type Triterpenoid Glycosides from the Rhizomes of *Hemsleya penxianensis* with Cytotoxic Activities. *Molecules*. 2019 Aug 13;24(16):2937. doi: 10.3390/molecules24162937.
7. Zeng Y, Wang J, Huang Q, Ren Y, Li T, Zhang X, Yao R, Sun J. Cucurbitacin IIa: A review of phytochemistry and pharmacology. *Phytother Res*. 2021 Aug;35(8):4155-4170. doi: 10.1002/ptr.7077.
8. Hunsakunachai N, Nuengchamnong N, Jiratchariyakul W, Kummalue T, Khemawoot P. Hunsakunachai N, Nuengchamnong N, Jiratchariyakul W, Kummalue T, Khemawoot P. Pharmacokinetics of cucurbitacin B from *Trichosanthes cucumerina* L. in rats. *BMC Complement Altern Med*. 2019 Jul 4;19(1):157. doi: 10.1186/s12906-019-2568-7.
9. Zhou SM, Guan SY, Yang L, Yang LK, Wang L, Nie HF, Li X, Zhao MG, Yang Q, Wu H. Cucurbitacin IIa exerts antidepressant-like effects on mice exposed to chronic unpredictable mild stress. *Neuroreport*. 2017 Mar 22;28(5):259-267. doi: 10.1097/WNR.0000000000000747.
10. Luo TT, Lu Y, Yan SK, Xiao X, Rong XL, Guo J. Network Pharmacology in Research of Chinese Medicine Formula:

- Methodology, Application and Prospective. *Chin J Integr Med*. 2020 Jan;26(1):72-80. doi: 10.1007/s11655-019-3064-0.
11. Kim S, Chen J, Cheng T, Gindulyte A, He J, He S, Li Q, Shoemaker BA, Thiessen PA, Yu B, Zaslavsky L, Zhang J, Bolton EE. PubChem 2023 update. *Nucleic Acids Res*. 2023 Jan 6;51(D1):D1373-D1380. doi: 10.1093/nar/gkac956.
 12. Daina A, Michielin O, Zoete V. SwissTargetPrediction: updated data and new features for efficient prediction of protein targets of small molecules. *Nucleic Acids Res*. 2019 Jul 2;47(W1):W357-W364. doi: 10.1093/nar/gkz382.
 13. Liu X, Ouyang S, Yu B, Liu Y, Huang K, Gong J, Zheng S, Li Z, Li H, Jiang H. PharmMapper server: a web server for potential drug target identification using pharmacophore mapping approach. *Nucleic Acids Res*. 2010 Jul;38(Web Server issue):W609-14. doi: 10.1093/nar/gkq300.
 14. Liu Z, Guo F, Wang Y, Li C, Zhang X, Li H, Diao L, Gu J, Wang W, Li D, He F. BATMAN-TCM: a Bioinformatics Analysis Tool for Molecular mechANism of Traditional Chinese Medicine. *Sci Rep*. 2016 Feb 16;6:21146. doi: 10.1038/srep21146.
 15. Rebhan M, Chalifa-Caspi V, Prilusky J, Lancet D. GeneCards: integrating information about genes, proteins and diseases. *Trends Genet*. 1997 Apr;13(4):163. doi: 10.1016/s0168-9525(97)01103-7.
 16. Amberger JS, Hamosh A. Searching Online Mendelian Inheritance in Man (OMIM): A Knowledgebase of Human Genes and Genetic Phenotypes. *Curr Protoc Bioinformatics*. 2017 Jun 27;58:1.2.1-1.2.12. doi: 10.1002/cpbi.27.
 17. Piñero J, Ramírez-Anguita JM, Sañch-Pitarch J, Ronzano F, Centeno E, Sanz F, Furlong LI. The DisGeNET knowledge platform for disease genomics: 2019 update. *Nucleic Acids Res*. 2020 Jan 8;48(D1):D845-D855. doi: 10.1093/nar/gkz1021.
 18. UniProt Consortium T. UniProt: the universal protein knowledgebase. *Nucleic Acids Res*. 2018 Mar 16;46(5):2699. doi: 10.1093/nar/gky092. Erratum for: *Nucleic Acids Res*. 2017 Jan 4;45(D1):D158-D169. doi: 10.1093/nar/gkw1099.
 19. Oliveros JC. VENNY. An interactive tool for comparing lists with Venn Diagrams. <http://bioinfogp.cnb.csic.es/tools/venny/index.html> 2007
 20. von Mering C, Jensen LJ, Snel B, Hooper SD, Krupp M, Foglierini M, Jouffre N, Huynen MA, Bork P. STRING: known and predicted protein-protein associations, integrated and transferred across organisms. *Nucleic Acids Res*. 2005 Jan 1;33(Database issue):D433-7. doi: 10.1093/nar/gki005.
 21. Chin CH, Chen SH, Wu HH, Ho CW, Ko MT, Lin CY. cytoHubba: identifying hub objects and sub-networks from complex interactome. *BMC Syst Biol*. 2014;8 Suppl 4(Suppl 4):S11. doi: 10.1186/1752-0509-8-S4-S11. Epub 2014 Dec 8.
 22. Dennis G Jr, Sherman BT, Hosack DA, Yang J, Gao W, Lane HC, Lempicki RA. DAVID: Database for Annotation, Visualization, and Integrated Discovery. *Genome Biol*. 2003;4(5):P3.
 23. O'Boyle NM, Banck M, James CA, Morley C, Vandermeersch T, Hutchison GR. Open Babel: An open chemical toolbox. *J Cheminform*. 2011 Oct 7;3:33. doi: 10.1186/1758-2946-3-33.
 24. Sehnal D, Bittrich S, Deshpande M, Svobodová R, Berka K, Bazgier V, Velankar S, Burley SK, Koča J, Rose AS. Mol* Viewer: modern web app for 3D visualization and analysis of large biomolecular structures. *Nucleic Acids Res*. 2021 Jul 2;49(W1):W431-W437. doi: 10.1093/nar/gkab314.
 25. Trott O, Olson AJ. AutoDock Vina: improving the speed and accuracy of docking with a new scoring function, efficient optimization, and multithreading. *J Comput Chem*. 2010 Jan 30;31(2):455-61. doi: 10.1002/jcc.21334.
 26. Abo-Zeid Y, Ismail NSM, McLean GR, Hamdy NM. A molecular docking study repurposes FDA approved iron oxide nanoparticles to treat and control COVID-19 infection. *Eur J Pharm Sci*. 2020 Oct 1;153:105465. doi: 10.1016/j.ejps.2020.105465.
 27. Pinzi L, Rastelli G. Molecular Docking: Shifting Paradigms in Drug Discovery. *Int J Mol Sci*. 2019 Sep 4;20(18):4331. doi: 10.3390/ijms20184331.
 28. Ferreira LG, Dos Santos RN, Oliva G, Andricopulo AD. Molecular docking and structure-based drug design strategies. *Molecules*. 2015 Jul 22;20(7):13384-421. doi: 10.3390/molecules200713384.
 29. Molloy PJ, Telford SR 3rd, Chowdri HR, Lepore TJ, Gugliotta JL, Weeks KE, Hewins ME, Goethert HK, Berardi VP. *Borrelia miyamotoi* Disease in the Northeastern United States: A Case Series. *Ann Intern Med*. 2015 Jul 21;163(2):91-8. doi: 10.7326/M15-0333.
 30. Beck AR, Marx GE, Hinckley AF. Diagnosis, Treatment, and Prevention Practices for Lyme Disease by Clinicians, United States, 2013-2015. *Public Health Rep*. 2021 Sep-Oct;136(5):609-617. doi: 10.1177/0033354920973235.
 31. Yu K, Yang X, Li Y, Cui X, Liu B, Yao Q. Synthesis of cucurbitacin IIa derivatives with apoptosis-inducing capabilities in human cancer cells. *RSC Adv*. 2020 Jan 23;10(7):3872-3881. doi: 10.1039/c9ra09113k.
 32. Zhao H, Dai X, Han X, Liu A, Bao F, Bai R, Ji Z, Jian M, Ding Z, Abi ME, Chen T, Luo L, Ma M, Tao L. *Borrelia burgdorferi* basic membrane protein A initiates proinflammatory chemokine storm in THP 1-derived macrophages via the receptors TLR1 and TLR2. *Biomed Pharmacother*. 2019 Jul;115:108874. doi: 10.1016/j.biopha.2019.108874.
 33. Cepok S, Zhou D, Vogel F, Rosche B, Grummel V, Sommer N, Hemmer B. The immune response at onset and during recovery from *Borrelia burgdorferi* meningoradiculitis. *Arch Neurol*. 2003 Jun;60(6):849-55. doi: 10.1001/archneur.60.6.849.
 34. Grygorczuk S, Czupryna P, Dunaj J, Moniuszko-Malinowska A, Świerzbńska R, Pancewicz S. The chemotactic cytokines in the cerebrospinal fluid of patients with neuroborreliosis. *Cytokine*. 2021 Jun;142:155490. doi: 10.1016/j.cyto.2021.155490.
 35. Ramesh G, Borda JT, Gill A, Ribka EP, Morici LA, Mottram P, Martin DS, Jacobs MB, Didier PJ, Philipp MT. Possible role of glial cells in the onset and progression of Lyme neuroborreliosis. *J Neuroinflammation*. 2009 Aug 25;6:23. doi: 10.1186/1742-2094-6-23.

*These authors contributed equally to the work.

**Correspondence:

Prof. Aihua Liu, Faculty of Basic Medical Sciences, Kunming Medical University, Kunming 650500, China. E-mail: liuaihua@kmmu.edu.cn
ORCID: 0000-0001-5726-6211.

Prof. Fukai Bao, Research Center, Baoshan People's Hospital, Baoshan 678100, Yunnan, China. E-mail: baofukai@kmmu.edu.cn
ORCID: 0000-0003-5726-6660.